Original Research

Beclin1- and Atg13-dependent autophagy activation and morroniside have synergistic effect on osteoblastogenesis

Xi Li[1]*, Yunrong Zhu[2]*, Xiangquan Lin[1], Chuanyuan Chen[1], Hui Liu[1] and Yi Shi[1]

[1]Department of Orthopedics, Fuzhou Second Hospital, Fuzhou 350007, China; [2]Department of Orthopedics, Affiliated Jiangyin Hospital of Nantong University, Jiangyin 214400, China
*Xi Li and Yunrong Zhu are considered as co-first authors
Corresponding authors: Yi Shi. Email: Shiyixmdx@163.com; Hui Liu. Email: 14730272@qq.com

Impact Statement

Osteoporosis is closely related to reduced osteoblastogenesis. Morroniside, as a main active component of iridoid glycosides from Cornus officinalis, serves in the treatment of osteoporosis, which is closely related to its promotion in osteoblastogenesis. However, during the process of treatment, morroniside promotes the mTOR activity of osteoblast precursors, which might lead to decreased autophagy, revealing a possible novel target for enhancing the pharmacological activity of morroniside. In this study, traditional pharmacological techniques and current gene intervention methods were used to reveal the significance of mTOR-autophagy signaling in osteoblastogenesis regulated by morroniside. Overall, we shed light on the improvement of therapeutic strategy of morroniside in osteoporosis: combining agents with autophagy-activating properties could be a potential choice for morroniside treatment, and Atg13 and Beclin1 may be promising mimic molecules of the above agents.

Abstract

Morroniside is known to improve osteoporosis by promoting osteoblastogenesis. The activation of PI3K/Akt/mTOR signaling is a significant mechanism in morroniside-promoted osteoblastogenesis. It is well known that protective autophagy is an important factor in osteoblastogenesis. However, the activation of mTOR signaling can inhibit autophagy. This study aimed to investigate the relationship between mTOR signaling and autophagy in morroniside-regulated osteoblastogenesis. In this study, we investigated the effect of morroniside on the autophagic activity (LC3 conversion rate, LC3-puncta formation, and autophagosome number) of differentiated osteoblast precursors (MC3T3-E1 cells). Then, we identified the roles of mTOR knockdown in morroniside-regulated alterations of autophagy and osteogenic parameters in MC3T3-E1 cells. Next, mTOR knockdown and overexpression were used to observe the roles of mTOR in morroniside-regulated alterations of autophagic molecules (Atg7, Atg13, and Beclin1). Subsequently, the additional value of the above autophagic molecules on morroniside-regulated osteogenic parameters in MC3T3-E1 cells was analyzed based on lentiviral transduction. Finally, combined with morroniside and TAT-Beclin1, the roles of Beclin1 upregulation in the *in vivo* effects of morroniside was investigated. Our experimental data showed that morroniside promoted both the mTOR activity and autophagy in MC3T3-E1 cells. Morroniside-upregulated autophagic activity and Atg13 or Beclin1 protein level in MC3T3-E1 cells were enhanced by mTOR knockdown. Furthermore, Morroniside-upregulated Atg13 and Beclin1 expression was reversed by mTOR overexpression. Importantly, autophagy upregulation with overexpression of the autophagic gene, Atg13 or BECN1 (gene form of Beclin1), significantly promoted osteoblastogenesis regulated by morroniside. The promotional effect of morroniside on bone microarchitecture, bone mass, and bone parameters (including trabecular bone area and OCN expression in trabecular bone) in ovariectomized (OVX) mice was enhanced by TAT-Beclin1 administration. In conclusion, the autophagy-enhancing drugs related to Beclin1 or Atg13 may be an effective adjuvant therapy in the treatment of osteoporosis with morroniside.

Keywords: Morroniside, Osteoblast, mTOR, Atg13, Beclin1

***Experimental Biology and Medicine* 2022; 247: 1764–1775. DOI: 10.1177/15353702221116879**

Introduction

The enhanced bone resorption caused by increased osteoclasts and impaired bone formation caused by decreased osteoblasts lead to bone loss, which is a core pathological basis of osteoporosis. Cornus officinalis (Shanzhuyu) is an herb and food plant used in traditional Chinese medicine, and its active components have been proven by many studies to have multiple pharmacological effects, such as anti-oxidant, anti-apoptosis, anti-inflammatory, anti-diabetes, anti-osteoporosis, and cardiovascular protection.[1] Morroniside is the main active component of iridoid glycosides from Cornus officinalis and also has a variety of biological activities.[2,3] Furthermore, morroniside plays a significant role in the treatment of osteoporosis, and it has been shown that morroniside inhibits bone loss. Lee *et al.*[4] elucidated

that morroniside could increase osteoblast formation and decrease osteoclast formation, thereby inhibiting ovariectomized (OVX)-induced osteoporotic pathogenesis in mice. This study revealed that morroniside could be an effective monotherapeutic compound for the prevention of osteoporosis.[4] Sun *et al*.[5] showed that *in vitro* high-glucose-impaired osteogenic differentiation of bone marrow mesenchymal stem cells (BMSCs) is reversed by treatment with morroniside. Morroniside can also reduce bone loss and improve bone microstructure *in vivo*.[5] In addition, morroniside can directly promote the differentiation and inhibit the apoptosis of osteoblast precursors.[6] Morroniside derivatives also have effects on the proliferation of osteoblast precursors and the expression of osteogenic markers.[7] Moreover, our research team found that morroniside can promote osteoblast formation via phosphoinositide 3-kinase/protein kinase B/mammalian target of rapamycin (PI3K/Akt/mTOR) signaling.[8] Accordingly, morroniside can effectively promote osteoblastogenesis and subsequent bone formation, thus improving osteoporosis.

Our team confirmed that PI3K/Akt/mTOR signal transduction is presented in morroniside-enhanced osteoblastogenesis.[8] The osteoblast differentiation promoted by morroniside can be reversed by the pharmacological inhibition of mTOR.[8] However, it should be noted that mTOR is a negative regulatory signaling of autophagy. The upstream stimulation can activate autophagy through the inhibition of mTOR signaling. Autophagy is a highly conserved intracellular homeostasis mechanism. Moderate autophagy is a protective mechanism, namely protective autophagy. Previous studies have also shown that there is a reverse relationship between PI3K/Akt/mTOR signaling and autophagy activation.[9–11] Nevertheless, as a mechanism of cell protection, autophagy plays an important role in osteoblastogenesis. Vidoni *et al*.[12] demonstrated that autophagy enhances osteogenic differentiation of human gingival mesenchymal stem cells. Weng *et al*.[13] also clarified that the silencing of the autophagic gene ATG5 can inhibit the proliferation and differentiation of osteoblasts. In addition, autophagy exerts a significant promoting effect on tantalum nanoparticle-induced osteoblast proliferation.[14] Furthermore, early autophagy can reduce the oxidative damage of osteoblasts caused by hydrogen peroxide via the endoplasmic reticulum stress pathway.[15] These results indicate that the positive effect of autophagy is involved in the early proliferation, differentiation, and survival protection of osteoblasts. Accordingly, we hypothesized that the mTOR activity promoted by morroniside may inhibit autophagy during treatment, which partly hinders its positive pharmacological effect. Therefore, it is of great significance to study the relationship among morroniside, mTOR signaling, and autophagy with osteoblasts as carriers.

In this study, we first investigated the effect of morroniside pharmacological intervention on autophagy of osteoblast precursors, MC3T3-E1. Next, we observed the effects of mTOR signaling inhibition on osteoblast precursor autophagy and osteoblastogenic parameters treated with morroniside. Ultimately, the relevant experiments were used to identify the effects of overexpression of corresponding autophagic molecules on morroniside pharmacological efficacy *in vitro* and *in vivo*.

Materials and methods

Cell line and culture

Mouse osteoblast precursor, MC3T3-E1 cell line, was purchased from American Tissue Culture Collection (ATCC); 293 cells were purchased from GeneCopoeia (Rockville, MD, USA). Cells were cultured in a humidified environment at 37°C and 5% CO_2.

Osteogenic induction and alkaline phosphatase (ALP) activity and mineralization capacity analyses

MC3T3-E1 cells were seeded into a 12-well plate at an initial number of 1×10^5 cells per well. In order to induce osteogenic differentiation, cells were initially incubated in basal growth medium and switched to osteoblast-inducing medium, containing 60 μg/mL ascorbic acid, 2 mM β-glycerophosphate and 10 nM dexamethasone (Sigma-Aldrich). After 7 days of differentiation induction, mature osteoblasts were evaluated using the corresponding ALP staining kit according to manufacturer's protocols (Beyotime, Jiangsu, China), and ALP activity was measured using a relevant kit according to manufacturer's protocols (Nanjing Jiancheng Bioengineering Institute, Jiangsu, China). After 7 days of induction, mineralization capacity was measured using Alizarin red staining. The treated cells were fixed with ice-cold 70% ethanol and stained with Alizarin red S to detect calcification according to manufacturer's protocols (Sigma-Aldrich). The quantitative parameters of the mineralized area were measured by detecting the percentages of positive areas using ImageJ 1.47 software.

Quantitative real-time PCR assays

Total RNA was extracted and purified by Trizol method. cDNA synthesis and quantitative real-time polymerase chain reaction (qRT-PCR) assays were carried out in accordance with manufacturer's protocols (Takara, Tokyo, Japan). The reaction was performed in 25 μL system, and reaction condition was as following: 50°C for 30 min, 94°C for 1 min, 57°C for 1 min, and 72°C for 7 min. Primer sequences of relevant genes are shown as follows:

mTOR, 5′-CTGATCCTCAACGAGCTAGTTC-3′ (sense) and
5′-GGTCTTTGCAGTACTTGTCATG-3′ (anti-sense);
PCNA, 5′-GAAGTTTTCTGCAAGTGGAGAG-3′ (sense) and
5′-CAGGCTCATTCATCTCTATGGT-3′ (anti-sense);
COL1, 5′-AGAACAGCGTGGCCT-3′ (sense) and
5′-TCCGGTGTGACTCGT-3′ (anti-sense);
OCN, 5′-AGCAGCTTGGCCCAGACCTA-3′ (sense) and
5′-TAGCGCCGGAGTCTGTTCACTAC-3′ (anti-sense);
Atg7, 5′-GTGTACGATCCCTGTAACCTAG-3′ (sense) and
5′-GATGCTATGTGTCACGTCTCTA-3′ (anti-sense);
Atg13, 5′-ACATCTTTTTCCACATCCCCTC-3′ (sense) and
5′-TGTTTAAGCCAGCAGTAAACAC-3′ (anti-sense);
BECN1, 5′-CTGGAGTCAGAGCTCGATATTT-3′ (sense) and
5′-GACAAGTTGCATGTAGTTGTGT-3′ (anti-sense);
GAPDH, 5′-ACCACAGTCCATGCCATCAC-3′ (sense) and
5′-TCCACCACCCTGTTGCTGTA-3′ (anti-sense).

Western blotting assays

The total protein was extracted using RIPA buffer (Solebao Technology Co., Ltd) and quantified using BCA kit (Solebao Technology Co., Ltd). About 15% SDS-polyacrylamide gel was used for loading and electrophoresis. The isolated proteins were then transferred to polyvinylidene fluoride (PVDF) membranes and incubated with rabbit anti-phosphorylated mTOR (p-mTOR; ser2448), LC3, mTOR, Atg7, Atg13, Beclin1, and glyceraldehyde 3-phosphate dehydrogenase (GAPDH) primary antibodies (Cell Signaling Technology, Boston, MA, USA) at 4°C overnight. Next, the membrane was incubated with the secondary antibody at room temperature for 60 min. Electrochemiluminescence (ECL) Kit (Millipore, Massachusetts, USA) was used to visualize the immunoreactive bands, and the ImageJ analyzer (NIH) was used to quantify the signals.

Immunofluorescence assays

Cells were inoculated on 6 cm dishes and fixed with 4% polytetrafluoroethylene (PFA). After perforation, the cells were blocked with 1% bovine serum albumin (BSA) and incubated with anti-LC3 antibody (1:500) overnight at 4°C. Subsequently, cells were stained with fluorochrome-labeled secondary antibody for 30 min, and then counterstained with 4′,6-diamidino-2-phenylindole (DAPI) for 15 min. Finally, the stained cells were visualized and recorded under fluorescence microscope (Olympus IX71, Tokyo, Japan). Cells containing more than five LC3-puncta are considered as positive cells.

Transmission electron microscope assays

The given cells were incubated on 6-cm dishes and treated with different treatments. The preparation of cell sections and staining were carried out in accordance with manufacturer's protocols. The ultrastructure of the samples fixed in 2.5% glutaraldehyde was visualized using the transmission electron microscope (TEM) according to the manufacturer's instructions (Hitachi, Tokyo, Japan).

siRNA transfection

Control siRNA or siRNA targeting mouse mTOR was obtained from Invitrogen. The target sequences were as follows:

Control, 5′-CGGATTGTCGGCCGTTCCTAAAGTT-3′.
mTOR, 5′-CGGAATAGTCTGGCCTGCTTCAGTT-3′.

The cells were incubated in six-well plates and then transfected with siRNA (100 pmol/well) using RNAiMAX (Invitrogen; Carlsbad, CA, USA) in accordance with manufacturer's protocols. Around 48 h later, endogenous mTOR level was detected via qRT-PCR and Western Blotting assays.

Lentiviral transduction

The recombinant lentivirus encoding *mTOR*, *ATG7*, *Atg13*, or *Beclin1* gene was constructed according to the manufacturer's instructions (GeneCopoeia) by homologous recombination between the expression vector (pEX-Puro-Lv105) and the cDNA in 293 cells using a lentivirus construction kit. The corresponding control vectors are constructed and packaged in the same way. Two days later, the supernatant was collected and MC3T3-E1 cells were cultured in the medium including lentivirus and 5 mg/L polybrene at an Multiplicity Of Infection (MOI) of 30 for 2 days. Puromycin (10 mg/L) was used to select the infected cells. Quantitative RT-PCR and Western Blotting assays were applied to identify the expression of each lentiviral gene.

Cell proliferation assays

Cell proliferation was evaluated using cell counting kit-8 (CCK-8) in accordance with manufacturer's protocols (Dojindo, Shanghai, China). The optical density at 450 nm (OD450) was measured via Varioskan Flash reader (Thermo Fisher Scientific, MA, USA).

Experimental scheme regarding TAT-Beclin1 peptide

TAT-Beclin1 peptide is known to induce autophagy.[16–18] The cell-permeable TAT-Beclin1 peptide was obtained from the Peptide Core of the University of Colorado Anschutz Medical Campus. The sequence of TAT-Beclin1 peptide is RRRQRRKKRGYGGDHWIHFTANWV.[16] In *in vivo* experiments, all mice were treated with TAT-Beclin1 or vehicle (normal saline) via intraperitoneal injection (i.p.) at a dose of 20 mg/kg/day.

OVX mice modeling

Around four- to eight-week-old C57BL/6 female mice were obtained from the Animal center of Gem Pharmatech Co., Ltd (Nanjing, China). The mice were placed in an ordinary environment with room temperature of 20–30°C and humidity of 60–80% and fed with ordinary laboratory feed. Bilateral ovariectomy was carried out in 10-week-old mice under ether anesthesia (6 mL; inhalation anesthesia). After three days, OVX mice were treated with morroniside (60 μg/kg/d) together with or without TAT-Beclin1. All above agents were injected intraperitoneally. Six weeks later, the tibiae were harvested, wrapped with gauze soaked in 0.9% salt water, and stored at −20°C. All mice were sacrificed via cervical dislocation. The sacrifice of mice was confirmed when the heart and breathing stopped. All protocols were approved by the Institutional Animal Care and Use Committee of Fuzhou Second Hospital, Fuzhou, China (approval id. 2019J01548). All mice were treated with morroniside (60 μg/kg/day) along with or without TAT-Beclin1 (20 mg/kg/day) via intraperitoneal injection (i.p.) for six weeks.

Micro-computed tomography

Three-dimensional (3D) reconstructions of the cancellous bones in the proximal tibia metaphysis were made using Bruker Micro-CT system (Skyscan1276, Kontich, Belgium). Scan settings are as follows: voxel size 6.533481 μm, medium resolution, 55 kV, 200 mA, 1 mm Al filter, and integration time 384 ms. The parameters involved bone mineral density (BMD), bone volume density (BV/TV), trabecular number (Tb.N), and trabecular separation/spacing (Tb. Sp) (N = eight/group).

Hematoxylin-eosin and immunohistochemical staining in bone tissue

Mouse tibiae were fixed in 4% PFA for 48 h, decalcified with 10% ethylenediaminetetraacetic acid (EDTA) (pH 7.3) at 4°C for two weeks, then dehydrated with graded ethanol and embedded in paraffin. Tibial sections (5-μm thick) were stained with hematoxylin and eosin (H&E) to observe the state of trabecular bone (N = six/group). Osteoblasts were semi-quantified *via* immunohistochemical (IHC) staining of corresponding sections (OCN, 1:200; Beclin1, 1:100; p-mTOR, 1:100; Abcam, Cambridge, UK) (N = six/group). The trabecular area (%Tb.Ar) of H&E-stained sections was analysed using Image-Pro Plus software (IPP, version 7.0). For IHC assays, all sections were incubated overnight in citrate buffer at 60°C to expose the antigens. Subsequently, the sections were incubated in the primary antibody at 4°C overnight and secondary antibody at room temperature for one hour. In IHC detection, the cytoplasm of trabecular positive cells was stained red.

Statistical analysis

Data are presented as the mean ± standard error of mean (SEM). All experiments were repeated at least three times. One-way or two-way analysis of variance (ANOVA) and Student's *t*-test were applied for statistical analyses. Bonferroni test was used for *post hoc* multiple comparisons of one-way or two-way ANOVA. At the threshold of $p < 0.05$, the difference was considered significant.

Results

Morroniside promoted mTOR and autophagy activities of osteoblast precursors

First, we investigated the effect of morroniside on the autophagy responses of MC3T3-E1 osteoblast precursors. Under the intervention of different concentrations of morroniside, mTOR phosphorylation level and LC3II protein expression increased in a concentration-dependent manner in MC3T3-E1 cells (Figure 1(A)). Moreover, morroniside upregulated the LC3 conversion rate (the ratio of LC3II to LC3I) and the formation of LC3-puncta in MC3T3-E1 cells in the presence and absence of the lysosomal protease inhibitor E64D plus pepstain A (Figure 1(B) to (D)). Based on the reality that treatment with lysosomal protease inhibitors enhanced the LC3 conversion and LC3-puncta formation of MC3T3-E1 cells, the experimental system is reliable (Figure 1(B) to (D)). In addition, morroniside administration significantly increased the number of autophagosomes in MC3T3-E1 cells (Figure 1(E) and (F)). These results suggested that morroniside can enhance the autophagy responses of osteoblast precursors.

mTOR silencing enhanced the promotional effect of morroniside on osteoblast precursor autophagy

We documented that morroniside enhanced both the mTOR activity and autophagy responses in osteoblast precursors. mTOR activity is known to be a negative factor in the autophagy activation. Accordingly, we explored whether mTOR inactivation and morroniside had a synergistic effect on enhancing autophagy of osteoblast precursors. The silencing efficiency of mTOR was verified using qPCR and Western blotting assays (Figure 2(A)). It was observed that both mTOR silencing and morroniside administration promoted the formation of LC3-puncta in MC3T3-E1 cells (Figure 2(B) to (D)). Moreover, the combination of mTOR silencing and morroniside resulted in more formation of LC3-puncta in MC3T3-E1 cells compared with the single intervention of morroniside (Figure 2(B) to (D)).

mTOR knockdown did not affect the effect of morroniside on osteoblastogenic parameters

Subsequently, the effect of mTOR inactivation on morroniside efficacy was observed. As shown in Figure 3(A) and (B), after morroniside intervention, the elevated ALP staining intensity and ALP activity in MC3T3-E1 cells were not reversed by mTOR silencing. In addition, the Alizarin red staining areas in MC3T3-E1 cells increased by morroniside was not reversed by mTOR silencing (Figure 3(C) and (D)). Furthermore, the proliferation of MC3T3-E1 cells enhanced by morroniside was not recovered by mTOR knockdown (Figure 3(E)). Consistently, the mRNA expression of proliferating cell nuclear antigen (PCNA), osteocalcin (OCN), and collagen type I (COL1) in MC3T3-E1 cells increased by morroniside was not reversed by mTOR silencing (Figure 3(F) to (H)). It was suggested that mTOR inactivation has no significant effect on the utility of morroniside in osteoblast formation.

Atg13 and Beclin1 were related to morroniside-mTOR-autophagy signaling in osteoblast precursors

We also need to identify the autophagic molecules related to morroniside-mTOR-autophagy signaling during osteoblastogenesis. As shown in Figure 4(A), morroniside increased the protein expression of Atg7 and Atg13 at 20 or 100 μM, while all concentrations of morroniside increased Beclin1 protein expression in MC3T3-E1 cells. In addition, mTOR silencing not only promoted the protein expression of Atg13 and Beclin1, but also further enhanced morroniside-promoted Atg13 and Beclin1 protein expression in MC3T3-E1 cells (Figure 4(B)). However, mTOR silencing had no effect on Atg7 protein expression in the absence and presence of morroniside (Figure 4(B)). Furthermore, mTOR overexpression not only inhibited Atg13 and Beclin1 protein expression, but also reversed morroniside-promoted Atg13 and Beclin1 protein expression in MC3T3-E1 cells (Figure 4(C)). Nevertheless, mTOR overexpression did not affect Atg7 protein expression in the absence and presence of morroniside (Figure 4(C)). mTOR overexpression not only inhibited LC3 conversion but also reversed morroniside-promoted LC3 conversion in MC3T3-E1 cells (Figure 4(C)), which confirmed the validity of our experimental system. These results indicated that Atg13 and Beclin1 are two molecules regarding morroniside-mTOR-autophagy signaling in osteoblast precursors.

Overexpression of BECN1 or Atg7 promoted the effect of morroniside on osteoblastogenic parameters

Ultimately, we examined the effects of autophagic gene overexpression on morroniside efficacy. The overexpression

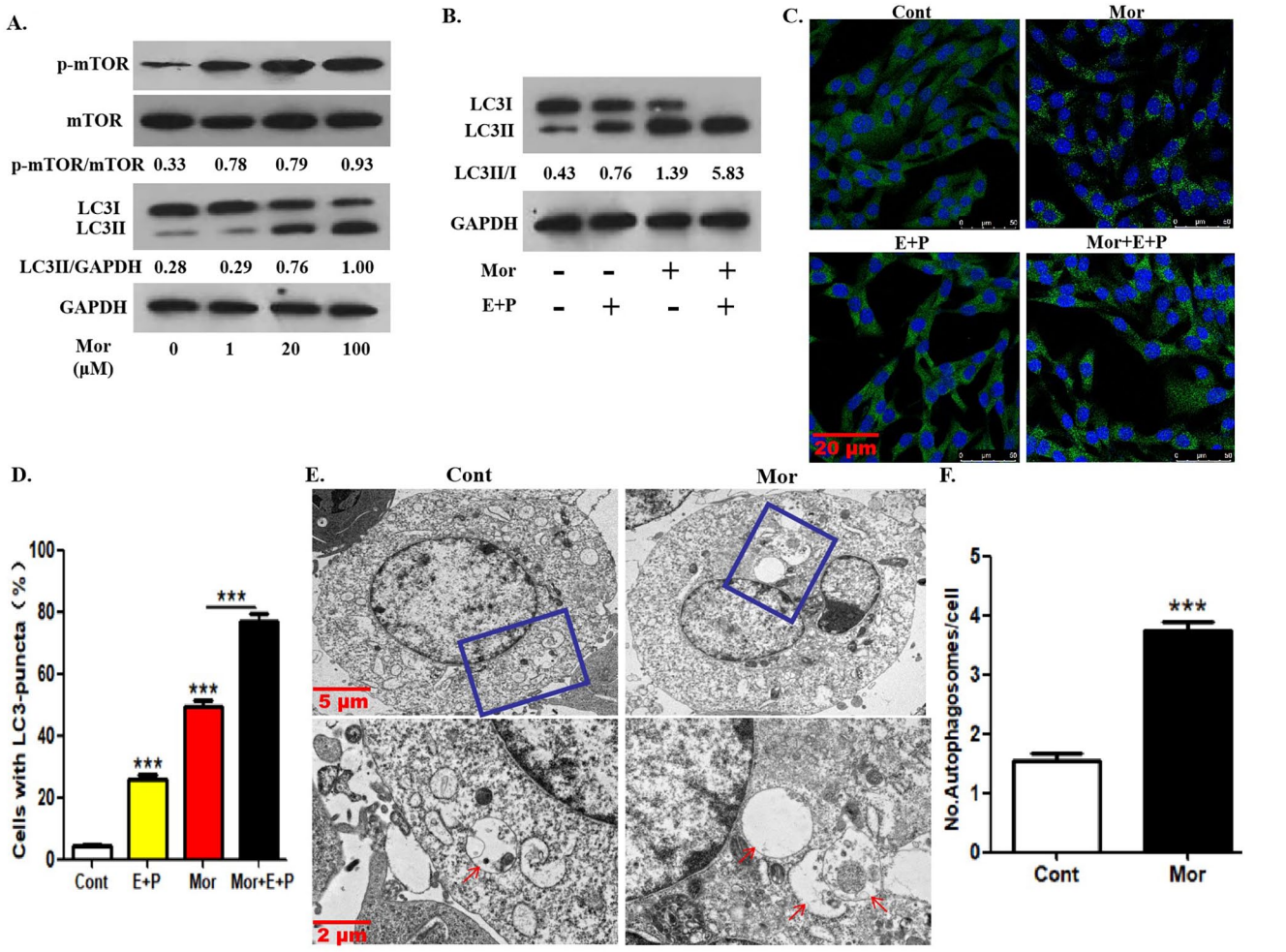

Figure 1. Morroniside promotes mTOR and autophagy of osteoblast precursors: (A) Following treated with different concentrations of morroniside for 24 h, mTOR phosphorylation level (p-mTOR) and LC3II protein expression in MC3T3-E1 cells were detected using Western blotting assays. (B) After treatment with morroniside (20 μM) or/and E64D plus Pepstain A for 12 h, LC3 conversion rate (LC3II/I) in MC3T3-E1 cells was detected using Western blotting assays. (C) After treatment with morroniside or/and E64D plus Pepstain A for 12 h, the formation of LC3-puncta in MC3T3-E1 cells was observed using fluorescence microscope. Scale bar, 20 μm. (D) The histogram shows the quantitative results of LC3-puncta-positive cells in C (40 cells per field, $N=5$). (E) After treatment with morroniside for 24 h, the formation of autophagosomes in MC3T3-E1 cells was observed under TEM. Scale bar, 5 μm or 2 μm. (F) The histogram shows the quantitative results of autophagosomes in E (45 cells in three independent experiments). Data are presented as mean ± SEM from three independent assays. ***$p < 0.001$. Cont, control group; Mor, morroniside; E, E64D; P, pepstain A. (A color version of this figure is available in the online journal.)

efficiencies of autophagic genes Atg7, BECN1, and Atg13 were verified using qPCR and Western blotting assays (Figure 5(A) and (B)). In addition, overexpression of three genes enhanced LC3 conversion of MC3T3-E1 cells in the presence of morroniside, among which BECN1 and Atg13 are far more effective than Atg7 (Figure 5(C)). As shown in Figure 5(D) to (G), ALP staining intensity, ALP activity and Alizarin red staining areas in MC3T3-E1 cells enhanced by morroniside were further promoted by overexpression of BECN1 or Atg13. Moreover, the upregulation of MC3T3-E1 cell proliferation induced by morroniside was further enhanced by the overexpression of BECN1 or Atg13 (Figure 5(H)). Consistently, the upregulation of PCNA, OCN, and Col1 mRNA expression in MC3T3-E1 cells induced by morroniside was further promoted by the overexpression of BECN1 or Atg13 (Figure 5(I) to (K)). However, overexpression of ATG7 is ineffective for the utility of morroniside in the above osteoblastogenic parameters (Figure 5(D) to (K)). These results suggested that the autophagy activation based on overexpression of BECN1 and Atg13 can amplify the efficacy of morroniside in osteoblastogenic activity.

Treatment of TAT-Beclin1 promoted the effect of morroniside on osteogenic indexes *in vivo*

We documented the role of autophagy activation in promoting the efficacy of morroniside *in vitro*. The effect of autophagy activation on morroniside's efficacy in osteogenesis *in vivo* also requires further investigation. We used the autophagy activator TAT-Beclin1 as a tool for *in vivo* experiments. First, IHC staining demonstrated that *in vivo* administration of morroniside enhanced the protein expression of p-mTOR, and the application of TAT-Beclin1 increased Beclin1 protein expression in the trabecular bone of OVX mice (Figure 6(A) and (B)). Micro-CT assays showed that morroniside improved the osteoporotic parameters of OVX mice. As shown in Figure 6(C), (F) to (I), morroniside administration ameliorated the bone microarchitecture and

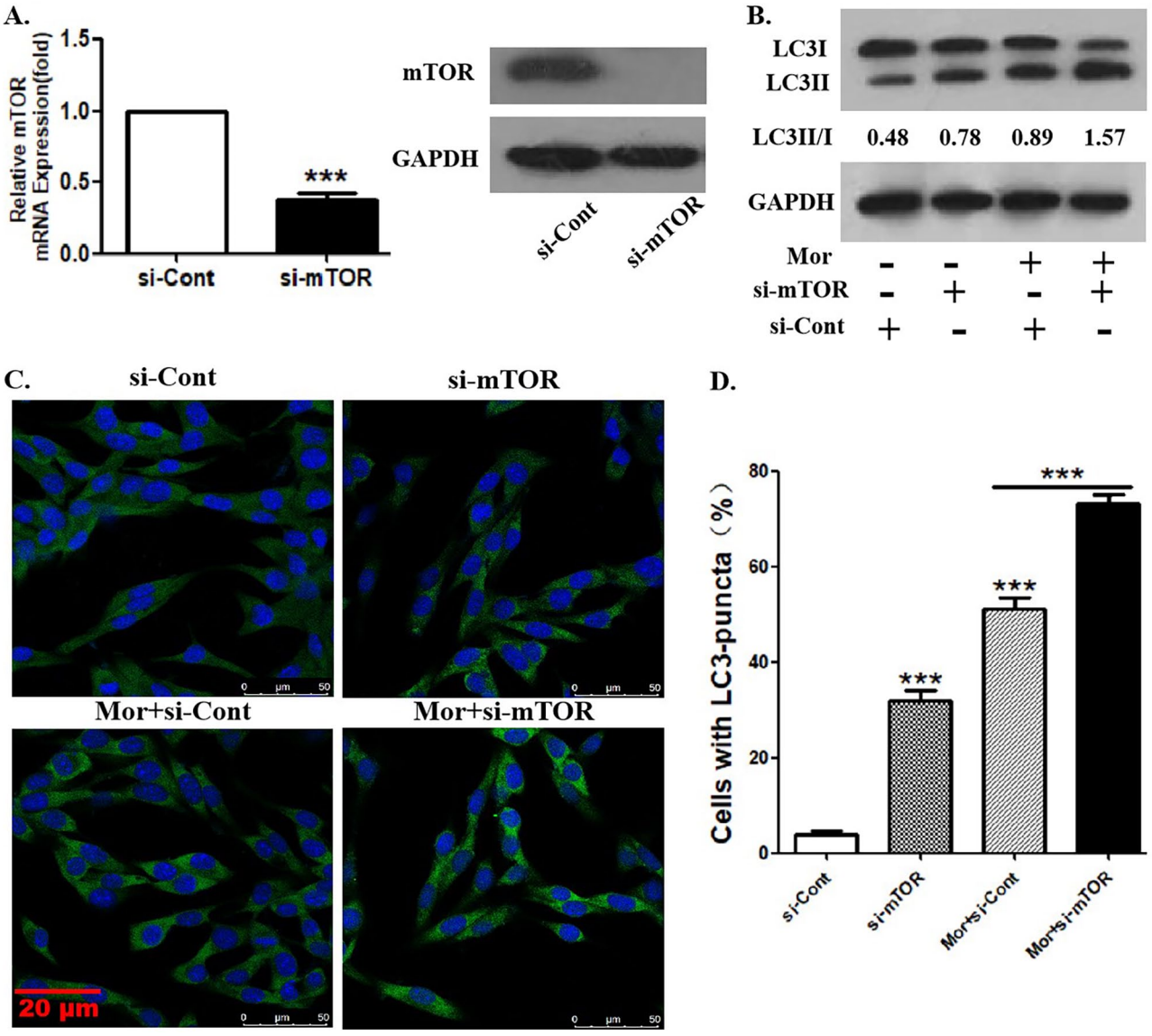

Figure 2. mTOR silencing enhances morroniside's effect on osteoblast precursor autophagy: (A) Following transfected with Control-siRNA (si-Cont) or mTOR-siRNA (si-mTOR), mRNA or protein level of mTOR in MC3T3-E1 cells was detected using qRT-PCR or Western blotting assays. (B) After treatment with morroniside for 12 h, LC3 conversion in MC3T3-E1 cells transfected with the given siRNAs was detected using Western blotting assays. (C) After treatment with morroniside for 24 h, the formation of LC3-puncta in MC3T3-E1 cells transfected with the given siRNAs was observed using fluorescence microscope. Scale bar, 20 μm. (D) The histogram shows the quantitative results of LC3-puncta-positive cells in C (40 cells per field, $N = 5$). Data are presented as mean ± SEM from three independent assays. ***$p < 0.001$. Mor, morroniside. (A color version of this figure is available in the online journal.)

increased BMD, BV/TV, and Tb.N and decreased Tb.Sp in OVX mice. After adding TAT-Beclin1, the regulatory effect of morroniside on the above parameters was further amplified (Figure 6(C), (F) to (I)). H&E staining showed that the phenotypes of bone loss in OVX mice, such as thinning of the growth plates, diminishing of bone trabeculae, and increase of bone marrow fat vacuoles, were ameliorated by morroniside administration, effects that were further optimized with the addition of TAT-Beclin1 (Figure 6(D)). The quantitative results regarding H&E staining showed that the slim trabecular area in OVX mice was increased by morroniside administration, an effect that was enhanced with the addition of TAT-Beclin1 (Figure 6(J)). More importantly, IHC assays showed that morroniside-increased trabecular OCN protein expression in OVX mice was enhanced by treatment with TAT-Beclin1 (Figure 6(E) and (K)). These results demonstrate the synergistic effect of autophagy activation and morroniside on bone improvement and osteoblastogenesis *in vivo*.

Discussion

As a major metabolic bone disease, osteoporosis is closely related to reduced osteoblastogenesis. Morroniside, as the active ingredient of Cornus officinalis, serves as an effective drug in the treatment of osteoporosis, which is closely related to the promotion of morroniside in osteoblastogenesis.[4–8] However, during the process of treatment, morroniside promotes the mTOR activity of osteoblast precursors,[8] which might lead to decreased autophagy, revealing a possible

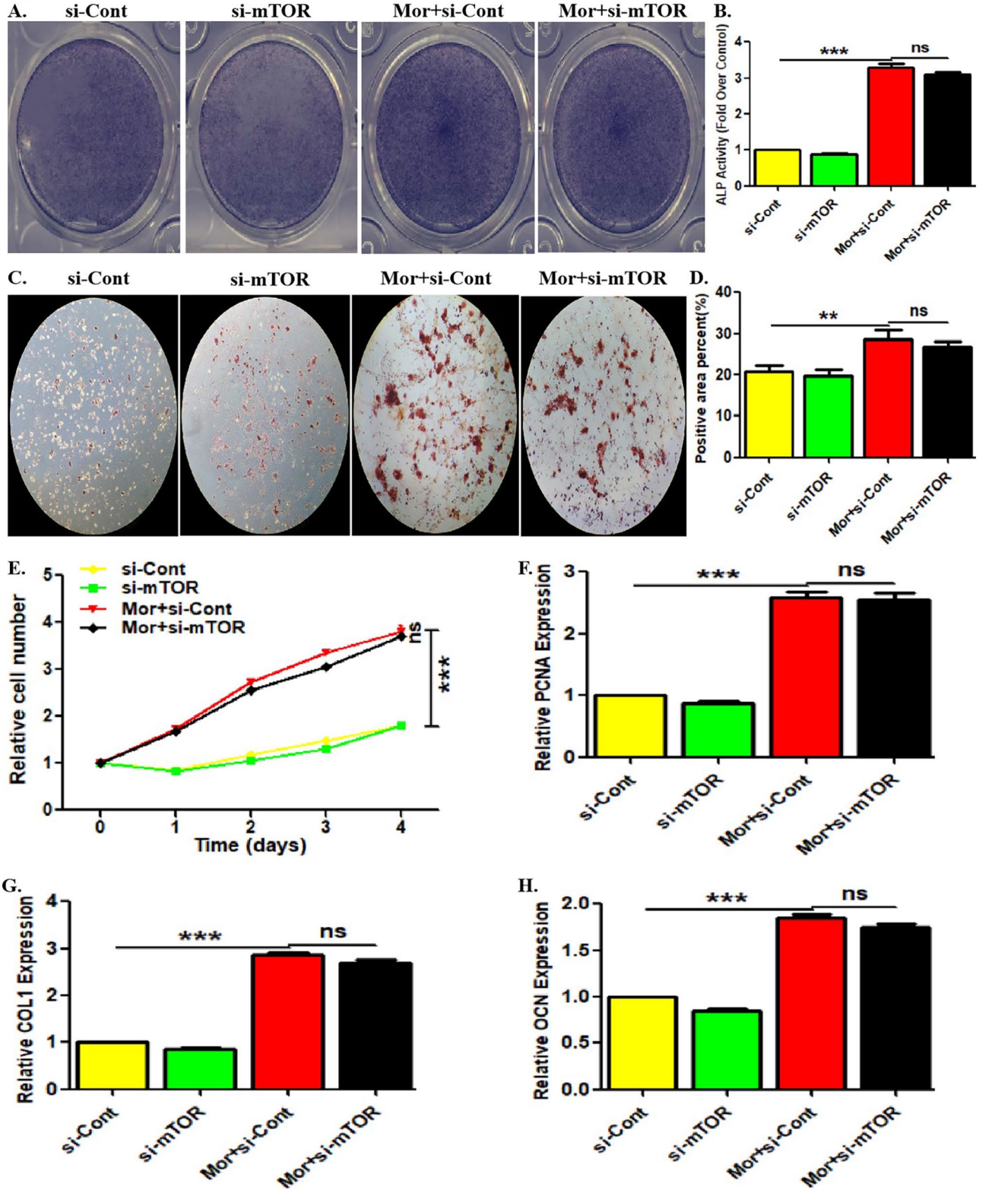

Figure 3. mTOR knockdown does not affect morroniside's effect on osteoblastogenesis: (A) and (B) After treatment with morroniside for 7 days in the presence of osteoblast-inducing reagents, osteoblastic differentiation level of corresponding MC3T3-E1 cells was assessed via ALP staining and measured by detecting ALP activity. (C) to (D) After treatment as described in A, mineralized nodules were detected by Alizarin red staining and quantified by ImageJ 1.47 software (five visible areas per group). (E) After treatment with morroniside for the indicated time in the presence of osteoblast-inducing reagents, the proliferation of corresponding MC3T3-E1 cells was evaluated using CCK-8 assays. (F) to (H) After treatment as described in A, mRNA levels of PCNA, COL1, and OCN in osteoblasts were detected using qPCR assays. Data are expressed as mean ± SEM from three independent experiments. ***$p < 0.001$. Mor, morroniside. (A color version of this figure is available in the online journal.)

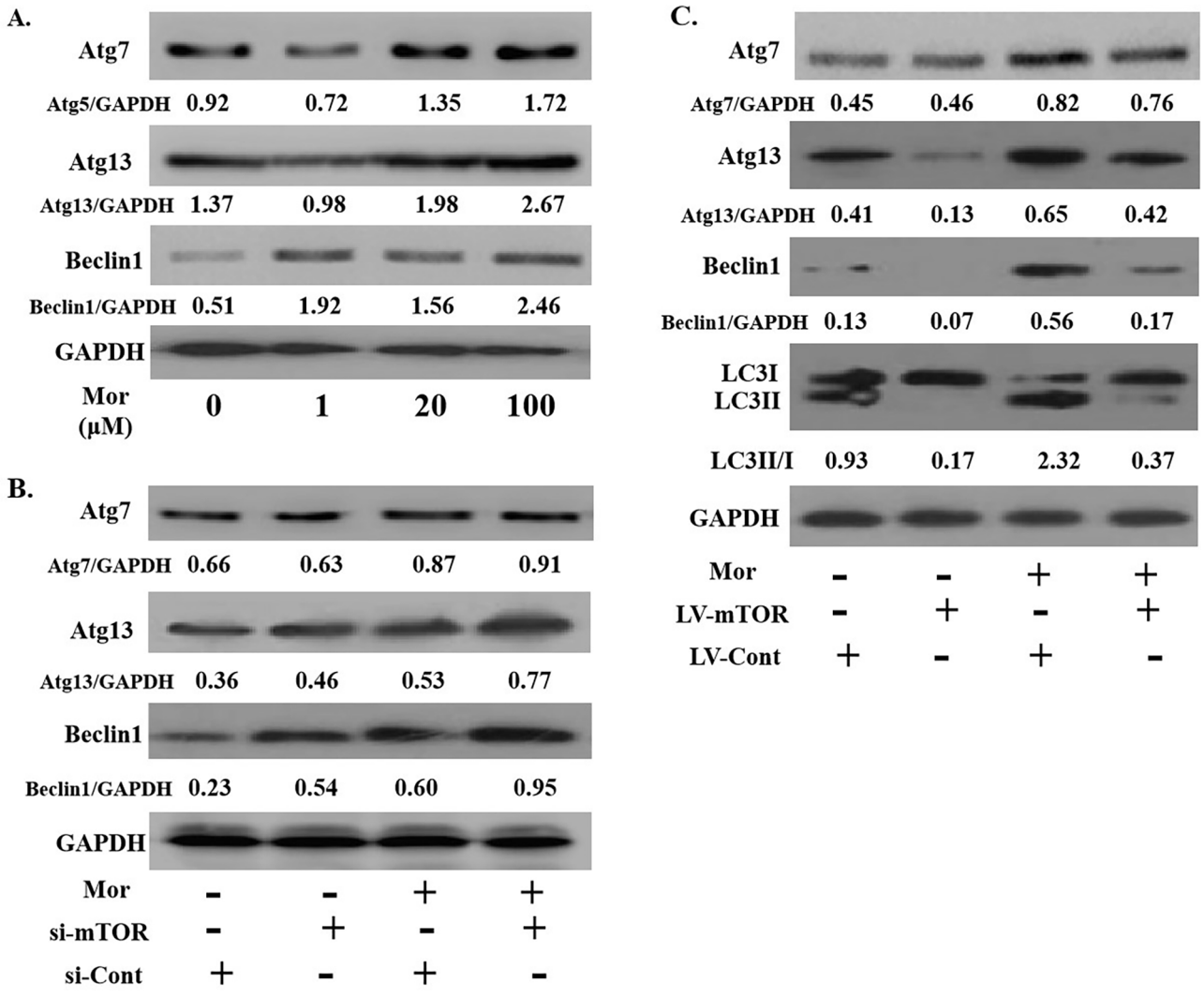

Figure 4. Atg13 and Beclin1 are related to morroniside-mTOR-autophagy signaling in osteoblast precursors: (A) after treatment with different concentrations of morroniside for 12 h in the presence of osteoblast-inducing reagents, the protein expression of Atg7, Atg13, and Beclin1 in MC3T3-E1 cells was detected using Western Blotting assays. (B) After treatment with morroniside for 12 h in the presence of osteoblast-inducing reagents, the protein expression of Atg7, Atg13, and Beclin1 in MC3T3-E1 cells transfected with the given siRNAs was detected using Western blotting assays. (C) After treatment with morroniside for 12 h in the presence of osteoblast-inducing reagents, the protein expression of Atg7, Atg13, and Beclin1 and LC3 conversion in MC3T3-E1 cells transduced with control vectors (LV-Cont) or expression vectors (LV-mTOR) were detected using Western blotting assays. Similar results were obtained in at least three repeated tests. (A color version of this figure is available in the online journal.)

novel strategy for enhancing the pharmacological activity of morroniside. In this study, traditional pharmacological techniques and current gene intervention methods were used to reveal the significance of mTOR-autophagy signaling in osteoblastogenesis regulated by morroniside.

Our experimental results showed that morroniside could activate the autophagic activity of osteoblast precursors, suggesting the promoting effect of morroniside on autophagy during osteoblastogenesis, which is similar to the research results of Gao *et al*.[19] in HO-induced podocytes. However, morroniside can promote both the mTOR activity and autophagy responses of osteoblast precursors. Moreover, mTOR gene silencing further enhanced the promotion of morroniside in autophagy of osteoblast precursors. These results indicated that the mTOR signaling activated by morroniside still leads to a certain degree of autophagy inhibition during osteoblastogenesis, which makes it possible for the synergistic effect of autophagy upregulation and morroniside to promote osteoblast precursor autophagy and osteoblastogenesis. It should be noted that during osteoblastogenesis, morroniside could activate autophagy even though it promoted mTOR activity. Therefore, morroniside may also enhance the autophagic activity of osteoblast precursors through other avenues, a possibility that is worthy of further exploration. Nevertheless, the genetic inactivation of mTOR exerted no further effect on osteoblastogenesis regulated by morroniside. This should be due to the dual role of mTOR signaling inhibition in promoting autophagy and inhibiting viability in osteoblast precursors. mTOR is a crucial signaling molecule that integrates internal and external signals and controls cell growth, metabolism, proliferation, and survival.[20,21] Moreover, mTOR signaling is known to function in osteoblastogenesis.[22–24] Remarkably, our team stated in a previous study that the pharmacological

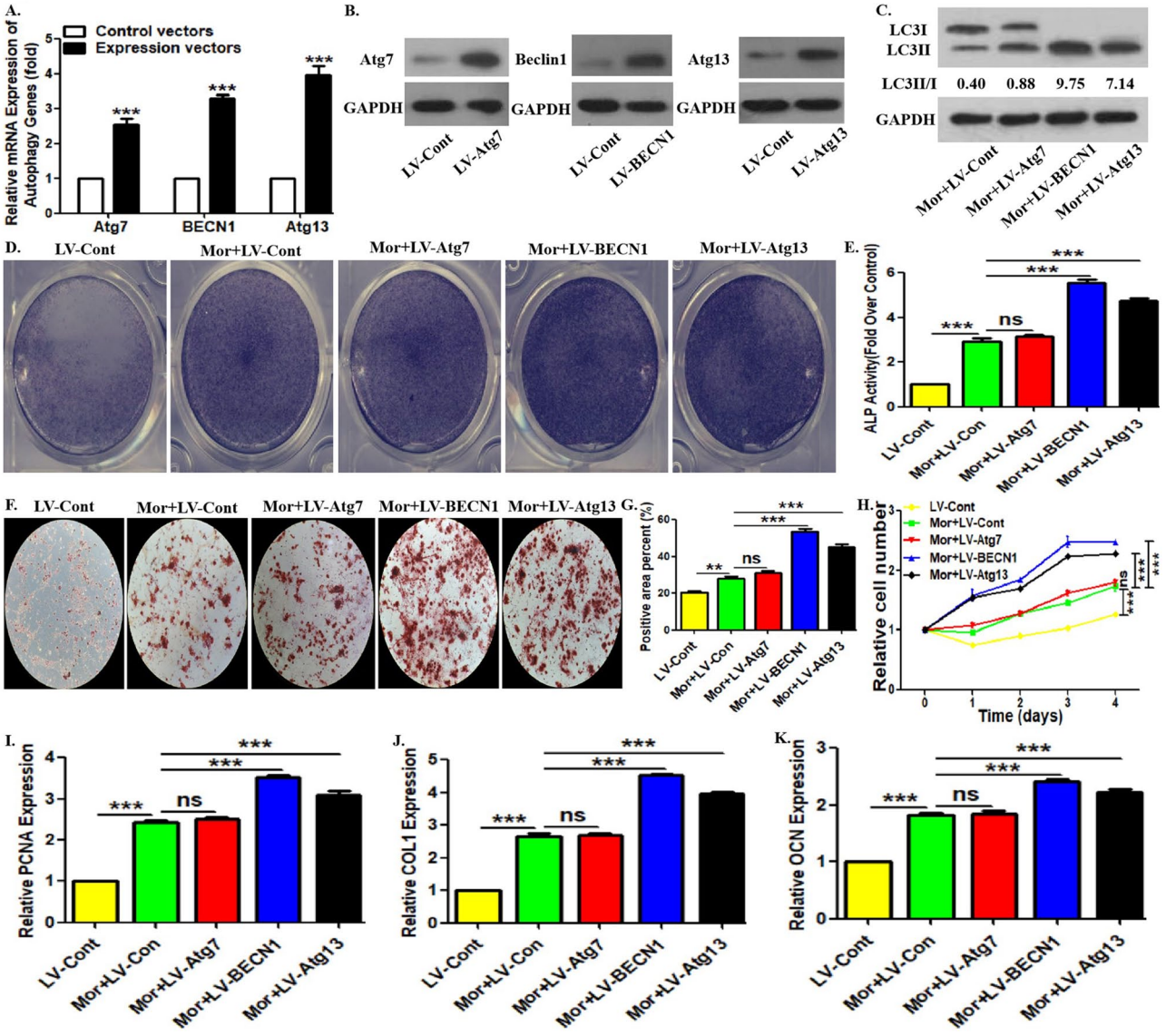

Figure 5. Atg7 or BECN1 overexpression promotes morroniside's effect on osteoblastogenesis: (A and B) Following transduced with control vectors (LV-Cont) or expression vectors (LV-Atg7, LV-Atg13, and LV-BECN1), mRNA or protein level of mTOR in MC3T3-E1 cells was detected using qRT-PCR or Western blotting assays. (C) After treatment with morroniside for 12 h in the presence of osteoblast-inducing reagents, LC3 conversion in lentiviruses-transduced MC3T3-E1 cells was detected using Western blotting assays. (D and E) After treatment with morroniside for seven days in the presence of osteoblast-inducing reagents, osteoblastic differentiation level from lentiviruses-transduced MC3T3-E1 cells was assessed via ALP staining and measured by detecting ALP activity. (F and G) After treatment as described in D, mineralized nodules were detected by Alizarin red staining and quantified by ImageJ 1.47 software (five visible areas per group). (H) After treatment with morroniside for the indicated time in the presence of osteoblast-inducing reagents, the proliferation of lentiviruses-transduced MC3T3-E1 cells was evaluated using CCK-8 assays. (I to K) After treatment as described in D, mRNA levels of PCNA, COL1, and OCN in osteoblasts were detected using qPCR assays. (A color version of this figure is available in the online journal.)

inactivation of mTOR could recover the enhanced osteoblastogenesis induced by morroniside.[8] The inconsistency between genetic and pharmacological manipulations may be attributed to the degree of autophagy activation related to mTOR activity inhibition. The genetic knockdown of mTOR may activate the protective autophagy of osteoblast precursors more effectively than mTOR pharmacological inactivation, thereby offsetting osteoblastogenesis suppressed by mTOR inhibition. The above inference is worthy of future exploration.

However, in contrast to mTOR inhibition, overexpression of the corresponding autophagic genes BECN1 and Atg13 significantly promoted the efficacy of morroniside on osteoblast precursor autophagy and osteoblast formation. Notably, although morroniside upregulated the protein expression levels of Atg7, Beclin1, and Atg13, mTOR expression alterations only resulted in changes in Beclin1 and Atg13 expression, including under morroniside intervention. Therefore, Atg13 and Beclin1 are two autophagic molecules related to morroniside-mTOR-autophagy signaling during osteoblastogenesis. mTOR is a central regulator of autophagy. Previous studies showed that Beclin1 and Atg13 are two key autophagic molecules downstream of mTOR, and mediate mTOR-regulated autophagy responses.[25,26] In addition, mTOR inhibition can lead to upregulation of Beclin1 and Atg13 expression.[26–32] Our data clarify that

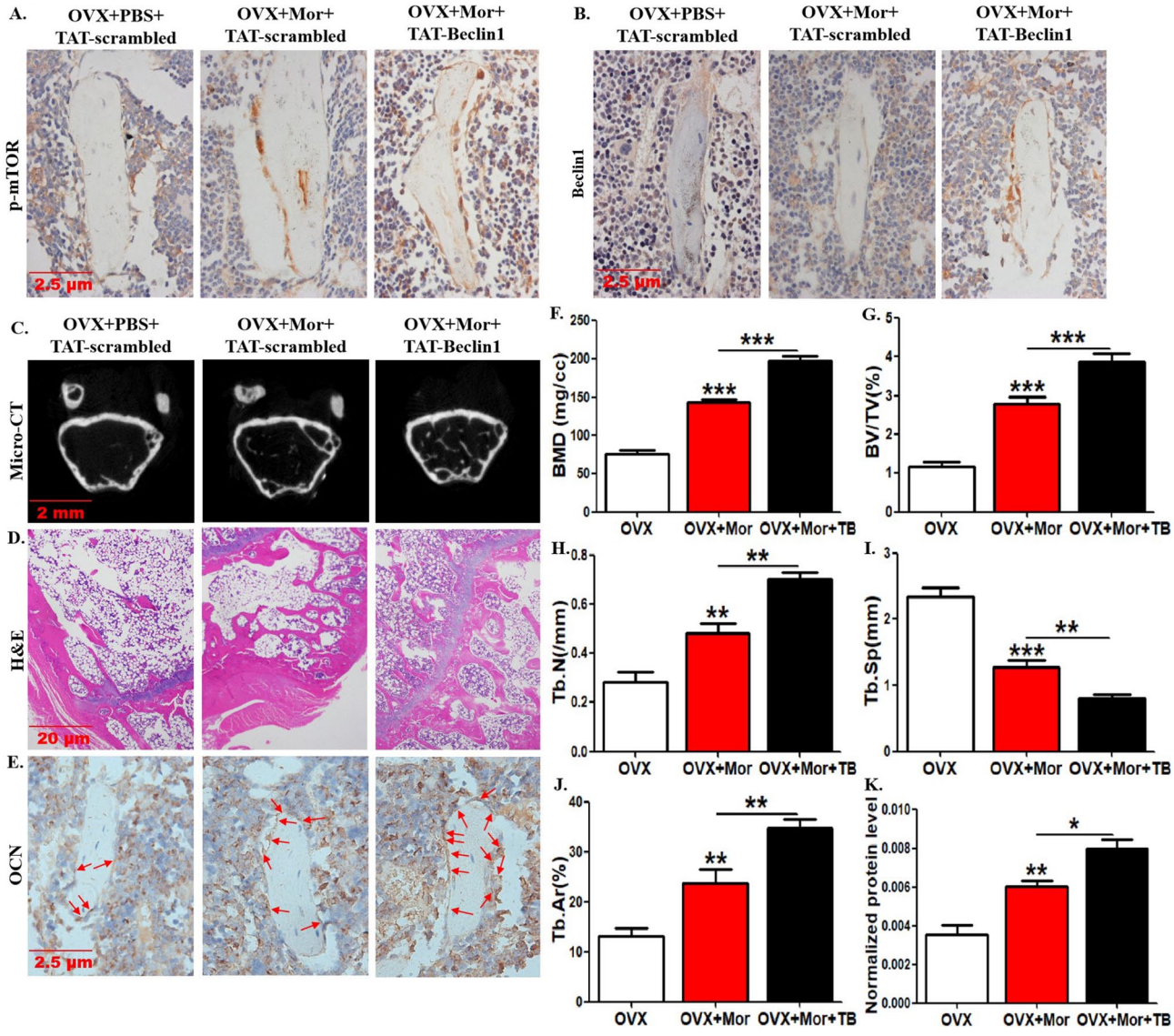

Figure 6. TAT-Beclin1 promotes morroniside's effect on osteogenesis *in vivo*. OVX-operated female mice were treated with morroniside (60 μg/kg/day) along with or without TAT-Beclin1 (20 mg/kg/day) for 6 weeks. (A and B) Representative IHC-stained tibial sections regarding p-mTOR and Beclin1 from each group. Scale bar, 2.5 μm. Similar results were obtained in the repeated tests of 6 mice. (C) Representative 3D Micro-CT reconstructed images of the tibiae from each group. Scale bar, 2 mm. (D) Representative H&E-stained tibial sections from each group. Scale bar, 20 μm. (E) Representative IHC-stained tibial sections regarding OCN from each group. Scale bar, 2.5 μm. (F to I) Micro-CT analyses showing trabecular bone parameters, including BMD, BV/TV, Tb.N and Tb.Sp (N = eight/group). (J) The trabecular bone area (%Tb.Ar) was analyzed by H&E staining and using the IPP system (N = six/group). (K) The histogram showing the quantitative results regarding IHC analyses (N = six/group). Data are expressed as the mean ± SEM. *$p < 0.05$; **$p < 0.01$; ***$p < 0.001$. OVX, mice treated with ovariectomy; Mor, morroniside; TB, TAT-Beclin1. (A color version of this figure is available in the online journal.)

under morroniside intervention, the expression of Atg13 and Beclin1 is not upregulated to full advantage due to mTOR activation, thus inhibiting autophagy of osteoblast precursors, which is an adverse factor of morroniside-promoted osteogenesis. Accordingly, due to the obvious compensation of autophagy inhibited by morroniside-mTOR signal transduction, the upregulation of Atg13 and Beclin1 can play a synergistic role with morroniside in promoting osteoblastogenesis. However, the concrete regulatory effect of morroniside or mTOR on the corresponding autophagic proteins needs to be clarified in the future. Remarkably, *in vivo* assays also indicated that a Beclin1 pharmacological activator could improve the efficacy of morroniside in improving bone loss and osteoblastogenesis in OVX mice, which further confirmed our *in vitro* experimental results. At present, there lacks specific peptide of other autophagic molecules, which limits our *in vivo* research. Therefore, the *in vivo* significance of other autophagic molecules in morroniside-regulated osteogenesis requires future exploration. Overall, the above results not only confirmed that mTOR activated by morroniside inhibited the autophagy of osteoblast precursors but also further identified the synergism of autophagy enhancement and morroniside in promoting osteoblastogenesis. The current working model regarding our study is described in Figure 7.

It has been confirmed that morroniside can promote osteoblast formation by activating mTOR signaling. However, mTOR exists as an inhibitory signal of autophagy, which

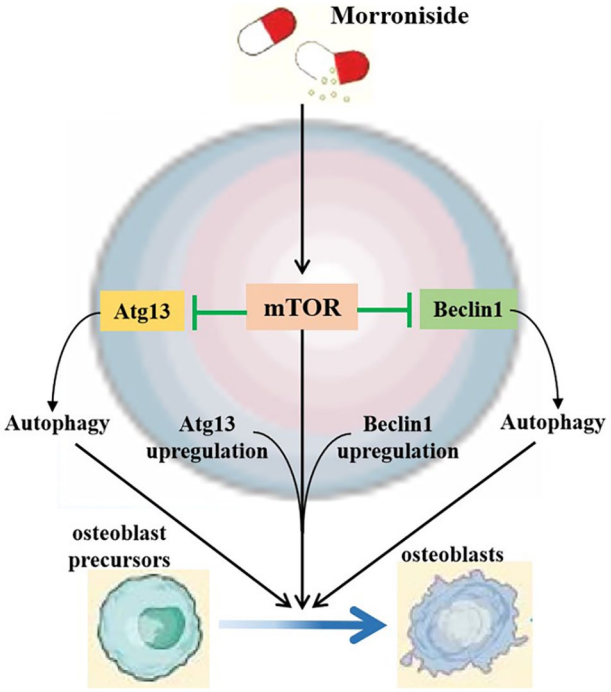

Figure 7. The working model regarding the role of mTOR-Beclin1/Atg13-autophagy signaling in morroniside-promoted osteogenesis. In brief, autophagy plays a significant role in the formation of mature osteoblasts derived from osteoblast precursors. Morroniside directly activates mTOR signaling, which contributes to osteoblastogenesis. However, mTOR activation leads to reduced expression of Beclin1 and Atg13, resulting in autophagy inhibition, which is not conducive to osteoblastogenesis. Accordingly, the upregulation of Beclin1 and Atg13 enhances morroniside's effect on promoting osteoblastogenesis. (A color version of this figure is available in the online journal.)

leaves a scientific question for our study: can the promotion of autophagy further enhance the efficacy of morroniside in treating osteoblastogenesis? Our research confirmed for the first time the significance of mTOR-autophagy signaling in morroniside-regulated osteoblast formation. In addition, we revealed two autophagic molecules related to morroniside-mTOR-autophagy inactivation in osteoblast precursors. Taken together, we shed light on the improvement of the therapeutic strategy of morroniside in osteoporosis: combining agents with autophagy-activating properties could be a potential choice for morroniside treatment, and Atg13 and Beclin1 may be promising mimic molecules of the above agents. Our findings will provide more clues for the better clinical application of morroniside in osteoporosis.

AUTHORS' CONTRIBUTIONS

Y.S., H.L., and X.L. conceived and designed experiments; X.L. and Y.Z. performed experiments, analyzed data, prepared figures, and helped with writing of the manuscript; X.Q.L. and C.Y.C. helped with experimental operation and data analysis; Y.S., H.L., and X.L. wrote the manuscript. D.S.K. reviewed and edited this manuscript. All authors have read and agreed to the published version of the manuscript.

DECLARATION OF CONFLICTING INTERESTS

The author(s) declared no potential conflicts of interest with respect to the research, authorship, and/or publication of this article.

FUNDING

The author(s) disclosed receipt of the following financial support for the research, authorship, and/or publication of this article: This work was supported by the Fujian Provincial Natural Science Foundation Projects (grant no. 2019J01548), Fujian Provincial Clinical Medical Research Center for First Aid and Rehabilitation in Orthopedic Trauma (grant no. 2020Y2014), and the Talent Training Project of Wuxi Taihu Lake (grant no. BJ2020103).

ORCID ID

Yi Shi https://orcid.org/0000-0002-9474-9383

REFERENCES

1. Gao X, Liu Y, An Z, Ni J. Active components and pharmacological effects of cornus officinalis: literature review. *Front Pharmacol* 2021;**12**:633447
2. Luo HR, Hattori H, Hossain MA, Hester L, Huang Y, Lee-Kwon W, Donowitz M, Nagata E, Snyder SH. Akt as a mediator of cell death. *Proc Natl Acad Sci U S A* 2003;**100**:11712–7
3. Huang JG, Xia C, Zheng XP, Yi TT, Wang XY, Song G, Zhang B. 17β-Estradiol promotes cell proliferation in rat osteoarthritis model chondrocytes via PI3K/Akt pathway. *Cell Mol Biol Lett* 2011;**16**:564–75
4. Lee CG, Kim J, Yun SH, Hwang S, Jeon H, Park E, Jeong SY. Anti-osteoporotic effect of morroniside on osteoblast and osteoclast differentiation in vitro and ovariectomized mice in vivo. *Int J Mol Sci* 2021;**22**:10642
5. Sun Y, Zhu Y, Liu X, Chai Y, Xu J. Morroniside attenuates high glucose-induced BMSC dysfunction by regulating the Glo1/AGE/RAGE axis. *Cell Prolif* 2020;**53**:e12866
6. Li M, Wang W, Wang P, Yang K, Sun H, Wang X. The pharmacological effects of morroniside and loganin isolated from Liuweidihuang Wan, on MC3T3-E1 cells. *Molecules* 2010;**15**:7403–14
7. Han H, Li Z, Qu N, Chen S, Dong P. Synthesis and promotion of the osteoblast proliferation effect of morroniside derivatives. *Molecules* 2018;**23**:1412
8. Liu H, Li X, Lin J, Lin M. Morroniside promotes the osteogenesis by activating PI3K/Akt/mTOR signaling. *Biosci Biotechnol Biochem* 2021;**85**:332–9
9. Chen W, Li Z, Duan J, Liu Y, Fang C, Bai Z. LncRNA SNHG6 inhibits autophagy of gastric carcinoma cells via PI3K/AKT/mTOR signaling pathway. *Am J Transl Res* 2022;**14**:2861–73
10. Maiello D, Varone M, Vicidomini R, Belli V, De Rosa M, Dama P, Furia M, Turano M. Dyskerin downregulation can induce ER stress and promote autophagy via AKT-mTOR signaling deregulation. *Biomedicines* 2022;**10**:1092
11. Yang L, Hu L, Tang H, Chen X, Liu X, Zhang Y, Wen Y, Yang Y, Geng Y. The disruption of human trophoblast functions by autophagy activation through PI3K/AKT/mTOR pathway induced by exposure to titanium carbide (Ti3C2) MXene. *Food Chem Toxicol* 2022;**165**:113128
12. Vidoni C, Ferraresi A, Secomandi E, Vallino L, Gardin C, Zavan B, Mortellaro C, Isidoro C. Autophagy drives osteogenic differentiation of human gingival mesenchymal stem cells. *Cell Commun Signal* 2019;**17**:98
13. Weng YM, Ke CR, Kong JZ, Chen H, Hong JJ, Zhou DS. The significant role of ATG5 in the maintenance of normal functions of Mc3T3-E1 osteoblast. *Eur Rev Med Pharmacol Sci* 2018;**22**:1224–32
14. Kang C, Wei L, Song B, Chen L, Liu J, Deng B, Pan X, Shao L. Involvement of autophagy in tantalum nanoparticle-induced osteoblast proliferation. *Int J Nanomedicine* 2017;**12**:4323–33
15. Yang YH, Li B, Zheng XF, Chen JW, Chen K, Jiang SD, Jiang LS. Oxidative damage to osteoblasts can be alleviated by early autophagy through the endoplasmic reticulum stress pathway: implications for the treatment of osteoporosis. *Free Radic Biol Med* 2014;**77**:10–20
16. Shoji-Kawata S, Sumpter R, Leveno M, Campbell GR, Zou Z, Kinch L, Wilkins AD, Sun Q, Pallauf K, MacDuff D, Huerta C, Virgin HW, Helms JB, Eerland R, Tooze SA, Xavier R, Lenschow DJ, Yamamoto A,

King D, Lichtarge O, Grishin NV, Spector SA, Kaloyanova DV, Levine B. Identification of a candidate therapeutic autophagy-inducing peptide. *Nature* 2013;**494**:201–6
17. Sun Y, Yao X, Zhang QJ, Zhu M, Liu ZP, Ci B, Xie Y, Carlson D, Rothermel BA, Sun Y, Levine B, Hill JA, Wolf SE, Minei JP, Zang QS. Beclin-1-dependent autophagy protects the heart during sepsis. *Circulation* 2018;**138**:2247–62
18. Atwood DJ, Pokhrel D, Brown CN, Holditch SJ, Bachu DM, Thorburn A, Hopp K, Edelstein CL. Increased mTOR and suppressed autophagic flux in the heart of a hypomorphic Pkd1 mouse model of autosomal dominant polycystic kidney disease. *Cell Signal* 2020;**74**:109730
19. Gao X, Liu Y, Wang L, Sai N, Liu Y, Ni J. Morroniside inhibits H2O2-induced podocyte apoptosis by down-regulating NOX4 expression controlled by autophagy in vitro. *Front Pharmacol* 2020;**11**:533809
20. Liu WJ, Luo MN, Tan J, Chen W, Huang LZ, Yang C, Pan Q, Li B, Liu HF. Autophagy activation reduces renal tubular injury induced by urinary proteins. *Autophagy* 2014;**10**:243–56
21. Hay N, Sonenberg N. Upstream and downstream of mTOR. *Genes & Development* 2004;**18**:1926–45
22. Linder M, Hecking M, Glitzner E, Zwerina K, Holcmann M, Bakiri L, Ruocco MG, Tuckermann J, Schett G, Wagner EF, Sibilia M. EGFR controls bone development by negatively regulating mTOR-signaling during osteoblast differentiation. *Cell Death Differ* 2018;**25**:1094–106
23. Singha UK, Jiang Y, Yu S, Luo M, Lu Y, Zhang J, Xiao G. Rapamycin inhibits osteoblast proliferation and differentiation in MC3T3-E1 cells and primary mouse bone marrow stromal cells. *J Cell Biochem* 2008; **103**:434–46
24. Zhang Z, Zhang X, Zhao D, Liu B, Wang B, Yu W, Li J, Yu X, Cao F, Zheng G, Zhang Y, Liu Y. TGF-β1 promotes the osteoinduction of human osteoblasts via the PI3K/AKT/mTOR/S6K1 signalling pathway. *Mol Med Rep* 2019;**19**:3505–18
25. Zhao E, Feng L, Bai L, Cui H. NUCKS promotes cell proliferation and suppresses autophagy through the mTOR-Beclin1 pathway in gastric cancer. *J Exp Clin Cancer Res* 2020;**39**:194
26. Su Y, Lu J, Chen X, Liang C, Luo P, Qin C, Zhang J. Rapamycin alleviates hormone imbalance-induced chronic nonbacterial inflammation in rat prostate through activating autophagy via the mTOR/ULK1/ATG13 signaling pathway. *Inflammation* 2018;**41**:1384–95
27. Tong X, Min W, Li S, Chen M, Song R, Bian J, Gu J, Liu Z. Beclin 1 positively regulates osteoprotegerin-induced inhibition of osteoclastogenesis by increasing autophagy in vitro. *Differentiation* 2021;**121**: 35–43
28. Tan P, Wang H, Zhan J, Ma X, Cui X, Wang Y, Wang Y, Zhong J, Liu Y. Rapamycin-induced miR-30a downregulation inhibits senescence of VSMCs by targeting Beclin1. *Int J Mol Med* 2019;**43**:1311–20
29. Rezabakhsh A, Ahmadi M, Khaksar M, Montaseri A, Malekinejad H, Rahbarghazi R, Garjani A. Rapamycin inhibits oxidative/nitrosative stress and enhances angiogenesis in high glucose-treated human umbilical vein endothelial cells: role of autophagy. *Biomed Pharmacother* 2017;**93**:885–94
30. Kuang P, Deng H, Liu H, Cui H, Fang J, Zuo Z, Deng J, Li Y, Wang X, Zhao L. Sodium fluoride induces splenocyte autophagy via the mammalian targets of rapamycin (mTOR) signaling pathway in growing mice. *Aging (Albany NY)* 2018;**10**:1649–65
31. Luo Z, Xu W, Ma S, Qiao H, Gao L, Zhang R, Yang B, Qiu Y, Chen J, Zhang M, Tao B, Cao F, Wang Y. Moderate autophagy inhibits vascular smooth muscle cell senescence to stabilize progressed atherosclerotic plaque via the mTORC1/ULK1/ATG13 signal pathway. *Oxid Med Cell Longev* 2017;**2017**:3018190
32. Martínez-Cisuelo V, Gómez J, García-Junceda I, Naudí A, Cabré R, Mota-Martorell N, López-Torres M, González-Sánchez M, Pamplona R, Barja G. Rapamycin reverses age-related increases in mitochondrial ROS production at complex I, oxidative stress, accumulation of mtDNA fragments inside nuclear DNA, and lipofuscin level, and increases autophagy, in the liver of middle-aged mice. *Exp Gerontol* 2016;**83**:130–8

(Received May 12, 2022, Accepted July 5, 2022)